Austin Journal of Environmental Toxicology

Open Access

Austin Publishing Group

Research Article

Physico-Chemical Characterization and Assessment of Cytotoxic and Genotoxic Effects of Poly-Ethylene-Glycol Coated and Uncoated Gold Nanoparticles on Human Kidney (HK-2) Cells

Rogers CR[1,2], Dasari S[1,2], Patlolla AK[1,2] and Tchounwou PB[1]*

[1]RCMI Center for Environmental Health, College of Science, Engineering and Technology, Jackson State University, USA

[2]Department of Biology, CSET, Jackson State University, USA

[3]Jackson Public School, USA

***Corresponding author:** Paul B Tchounwou, Presidential Distinguished Professor & Director, RCMI Center for Environmental Health, Jackson State University, Jackson, MS, USA

Received: November 12, 2021; **Accepted:** December 06, 2021; **Published:** December 13, 2021

Abstract

Although gold Nanoparticles (Au-NPs) have been widely used in medicine for the diagnosis and treatment of patients due to their unique physicochemical properties, chemical stability and biocompatibility, recent reports have also highlighted their potential to induce toxicity to humans. In the present study, we investigated the toxic effects of uncoated and Polyethylene Glycol (PEG)-coated AuNPs on human kidney (HK-2) cells. Both forms of AuNP were synthesized and characterized using standard protocols. Dynamic Light Scattering (DLS), Zeta Sizer Nano ZS analyzer, Transmission Electron Microscopy (TEM), and Inductively Coupled Plasma-Optical Emission Spectroscopy (ICP-OES) were used to measure their distribution, zeta potential/surface charge, morphological size, and Au concentrations, respectively. Cytotoxicity was measured by Cyto-Tox assay and trypan blue exclusion test. Oxidative Stress (OS) was assessed by quantifying the levels of Glutathione (GSH), and Mitochondria Membrane Potential (MMP). Genotoxicity was assessed by single cell gel electrophoresis (Comet assay) and Chromosomal Aberration (CA) assay. Uncoated AuNPs significantly reduced cell viability, increased ROS, decreased GSH, depolarized the MMP, and induced significant DNA damage and chromosomal alterations including chromosome gaps, centric rings, breaks, deletions, and intra and inter-chromosome exchanges, in a concentration-dependent manner. PEG-coated AuNPs displayed lower cytotoxic and genotoxic effects, and did not produce any significant increase in ROS or significant decrease in GSH along with negligible polarization of the MMP. Hence, PEG-coated AuNPs are relatively less toxic than uncoated AuNPs and therefore, may have potential applications in nanomedicine.

Keywords: AuNP polymer formulations; Cell viability; Oxidative stress; Cytotoxicity; Genotoxicity; HK-2 cells

Introduction

Gold Nanoparticles (AuNPs) are reported to have many biomedical and biotechnological applications including their incorporation into several diagnostic and therapeutic strategies in biology and medicine. AuNPS have been very useful not only in diagnosis of certain chronic diseases like cancer but also beneficial in treatment [1-6]. AuNPs have been extensively used due to their dynamic physical and chemical properties; however, this activity has been a public health concern [7]. Published research has demonstrated that nanoparticles can be absorbed and exhibit a long residence time with a big half-life because of the physico-chemical characteristics associated with nanosizes, shapes, and surface charges that increase their resistance to attack by the body's immune system. Therefore, toxicological implications of AuNPs appears to be a major disquietude, limiting their utilization for diagnosis and treatment of chronic health conditions.

It is generally believed that AuNPs are relatively noncytotoxic, however, there are differing reports alluding to the potential toxicity associated with their physico-chemical characteristics. Primarily, several *in vitro* studies of NPs have confirmed that their toxic potential is associated with their specific particle sizes [8-11]. Size of a nanoparticle is directly linked to its function. In addition, studies on surface chemistry of AuNPs reveal novel issues on their cytotoxic potential. Small AuNPs have larger surface area exhibiting high reactivity compared to larger size AuNPs with lower adsorption and reactivity. Such feature is the fundamental factor for AuNP application in nanotechnology. Because of their size, smaller AuNPs enter the cells more rapidly and once internalized, they may interact with many cellular components to cause biological effects. The molecular mechanism of their cytotoxicity is via triggering of apoptosis signaling pathway by inducing oxidative stress (ROS) [12,13]. Studies confirm that AuNPs induce oxidative stress leading to ROS production, lipid peroxidation and apoptotic mediated cell death [14,15]. Next, surface charge constitutes one of the key factors that modulate AuNPs toxicity. It is commonly determined by measuring the zeta potentials which help in assessing the stability of nanomaterials based on whether or not their charges are positive or negative. According to

Citation: Rogers CR, Dasari S, Patlolla AK and Tchounwou PB. Physico-Chemical Characterization and Assessment of Cytotoxic and Genotoxic Effects of Poly-Ethylene-Glycol Coated and Uncoated Gold Nanoparticles on Human Kidney (HK-2) Cells. Austin J Environ Toxicol. 2021; 7(2): 1042.

Platel et al. [16] information on surface charge is important to explain uptake mechanisms that would assist in predicting likely biological interactions that would be either protective or harmful.

The kidneys function primarily to remove metabolic waste such as urea and ammonia from the body. In addition, it has been reported that the kidneys may play a role in the excretion of other waste products including toxic metals, and Nanomaterials (NMs) [17]. The kidneys are highly vascularized and receive about 20% of blood coming from the heart. Kidneys are highly sensitive to nanoparticle-mediated toxicity due to their physiological activity in excretion of waste materials from human body. Hence, the major anatomical components of the kidneys including glomerular structures and tubular epithelial cells may be adversely affected by NMs. Because of their key role in the excretory system and their vulnerability to toxic chemicals, the kidneys represent important targets and test models for studying the deleterious effects of potential nephrotoxicants including nanomaterials. Hence, scientific reports show that kidneys act as target for nanomaterial toxicity [18].

However, AuNPs toxicity can be highly modulated by functionalized surface agents. Polymeric ligands improve the long-term stability of AuNPs and increase hydrophilicity of the surface. These nanoparticle-polymer formulations not only help in target site specificity but also enhance the circulation time in the blood [19]. In order to reduce the toxic side effects of AuNPs, coating agents like Polyethylene glycol (PEG) have been used [20-23]. Nanoparticle coating will increase the biocompatibility by modification of their surface to water solubility and other factors. To improve the stability and solubility of nanoparticle by conjugation with a polymer like PEG has been successful as it prevents aggregation, opsonization and enzyme degradation [24].

Therefore, the specific aims of this research were to synthesize and characterize PEG-coated and uncoated AuNPs using analytical methods such as TEM, zeta potential, dynamic light scattering and ICP-OES, and to assess their cytotoxicity and genotoxicity to human kidney (HK-2) cells.

Materials and Methods

Cells and culture media

Human Kidney (HK-2) epithelial cells, streptomycin (10000U/ml) and penicillin (10000U/ml) were purchased from the American Type Culture Collection (ATCC) (Manassas, VA, USA). Cells grown in DMEM/F12 (Dulbecco's Modified Eagles Medium) supplemented with fetal bovine serum (FBS) were purchased from ThermoFisher (Life Technologies) (Suwanee, GA, USA).

Synthesis of gold nanoparticles (AuNPs)

For the synthesis of uncoated AuNPs 3.75mL of Au chloride was added to boiling nanopure water for one hour. A reducing agent, (1% Trisodium Citrate) was added and allowed to cool for 10 min then centrifuge for three hours at 5,000 rpm. For the synthesis of PEG-coated nanospheres, AuNPs were conditioned with 0.5% vol ethanol and then immersed in the dispersion media. They were then mixed by sonication for 20 min and 8% of emulsifying solution contain 4% each of Polyoxyethylene Glycerol Trioleate and Tween 20 was used to create a more stable and biocompatible structure.

Size determination of gold nanoparticles

The size and distribution of AuNPs in ultrapure water were measured by dynamic light scattering (DLS), using Malvern Zetasizer Nano-ZS (Malvern Instruments Ltd., Worcestershire, UK). Transmission electron microscopy (TEM) was performed to characterize the studied nanoparticles. The preparation and examination of AuNPs on TEM were conducted as previously described by Patlolla et al. [25].

Elemental analysis of gold nanoparticles composition

HK-2 cells treated with AuNPs were analyzed by Inductively Coupled Plasma-Optical Emission Spectroscopy (ICP-OES) using a Perkin Elmer ICP-OES Optima 8000 DV available in our Environmental Toxicology Research Laboratory at Jackson state University. Sample preparation, and spectral collection and analysis of gold content were performed following the protocol described by Schmidt et al. [26].

Physicochemical properties of AuNPs

Zeta potential (ζ-potential) measurements were performed on both coated and uncoated AuNP using Malvern Instruments' Zetasizer Nano ZS. Sample preparation and instrumental analysis were carried out following the analytical protocol previously described in our laboratory [27].

Cell treatment with gold nanoparticles

The experiments were conducted in 96-well plates with three replicates for each positive control, negative control, non-cell control (serum free growth media without cells) and treatment sample of PEG coated and uncoated AuNP. 1x106 cells/mL was used for both controls and AuNP-treated cells. In order to determine AuNPs toxicity and their LC50 values, 6.25, 12.5, 25, 50, 100 and 200 μM NP were prepared in serum free DMEM//F12 media. All samples were kept for 24 hours at in a humidified 5% CO2 incubator at 37°C.

Measurement of cell viability and cytotoxicity

The cell viability was assessed by the trypan blue exclusion test using Nexcelom cellometer (Lawrence, MA, USA). This assay reflects all treatment-related effects (necrosis, cell-cycle delay, and apoptosis) that reduce the number of living cells, as described by Bumah et al. [28]. Results were expressed as the percentages of cell viability in treated cells compared to the negative control.

Cyto Tox-Glo assay

Cyto tox-Glo assay describe by Niles et al [29] determines cell mortality by measuring the amount of stable protease activity being release into the cell culture medium. The luminescence reflecting the number of viable cells was assessed as previously described [30].

ROS analysis using 2',7'-dichlorofluorescein (H2DCF)

ROS levels were determined using 2', 7'-dichlorofluorescein (H2DCF) obtained from Sigma Company. After incubation the cells were treated with H2DCF and spectrophotometric measurements of ROS were taken at 530nm following the procedure previously described by Skalska et al. [31].

Measurement of glutathione (GSH)

GSH-Glo Glutathione luminescence-based assay (Promega, Madison, WI, USA) was conducted to detect and quantify glutathione

in controls and AuNP-treated cells. This process involved seeding a 96-well tissue culture flask with 100µL aliquots containing 104 cells per well and incubating for 24 hours. A standard curve with a GSH range of 0-5 µM was generated by diluting 5mM Glutathione stock solution (1:100) in distilled water. The complete assay was performed according to the protocol instructions (Technical Manual TM344 - GSH/GSSG-Glo assay V6611) from Promega Corporation (Madison, Wisconsin, USA).

Measurement of mitochondrial membrane potential (Δψm)

5x 104 cells were placed in each well of a 96 well black-sided plate, and kept overnight to allow attachment, and subsequently washed one time with the dilution buffer. The fluorescence of each sample was read using an Omega Polarstar platform-reader with an excitation wavelength of 535±17.5 nm and an emission wavelength of 590±17.5 nm. The calculations and data analysis were conducted following the manufacturer's protocol [32].

Assessment of genotoxicity

Comet assay: Genotoxicity in AuNP-treated and untreated HK-2 cells was assessed by alkaline gel electrophoresis using Comet assay kit for single cell gel electrophoresis from Trevigen (Gaithersburg, MD, USA). Both controls and treated cells were analyzed for DNA damage following the Comet Assay protocol by Kermanizadeh [33]. The data were evaluated using the DNA damage analysis software (Loats Associates Inc., USA).

Chromosome aberration assay: Chromosome aberration was assessed using a previously described standard protocol [34]. A maximum of 200 cells of best quality metaphase spread of each treatment were captured and 100 cells of each treatment were scored manually using an Olympus microscope with a 10x magnification. Various types of chromosomal aberrations such as breaks, dicentrics, rings, and chromatid breaks were scored and analyzed for each treatment group.

Statistical analysis

Triplicate experiments were performed, and the data were expressed as means ± SDs. Using SAS 9.1 software, assessment of differences in mean values between controls and AuNP-treated cells was done by one-way analysis of variance (ANOVA) for multiple comparisons or Student's t-test for paired groups. Statistically significant differences were noted for p-value less than 0.05.

Results

Characterization of AuNPs

The nanoparticles that were characterized included Polyethylene Glycol (PEG) coated and uncoated and gold nanoparticles. Their size distribution and morphology were respectively characterized by DLS and TEM analysis (Figure 1). Data generated from this analysis indicated that the size of both forms of gold nanoparticles ranged from 20-25 nm (Table 1) and their shape was spherical. Dynamic Light Scattering (DLS) was used to determine average aggregate hydrodynamic diameters. Since light scattering is exponentially proportional to NP size, we have reported our DLS data as percentages of total volume and not percentages of measured intensity. Using this technique, we observe a 5nm increase in the hydrodynamic diameter

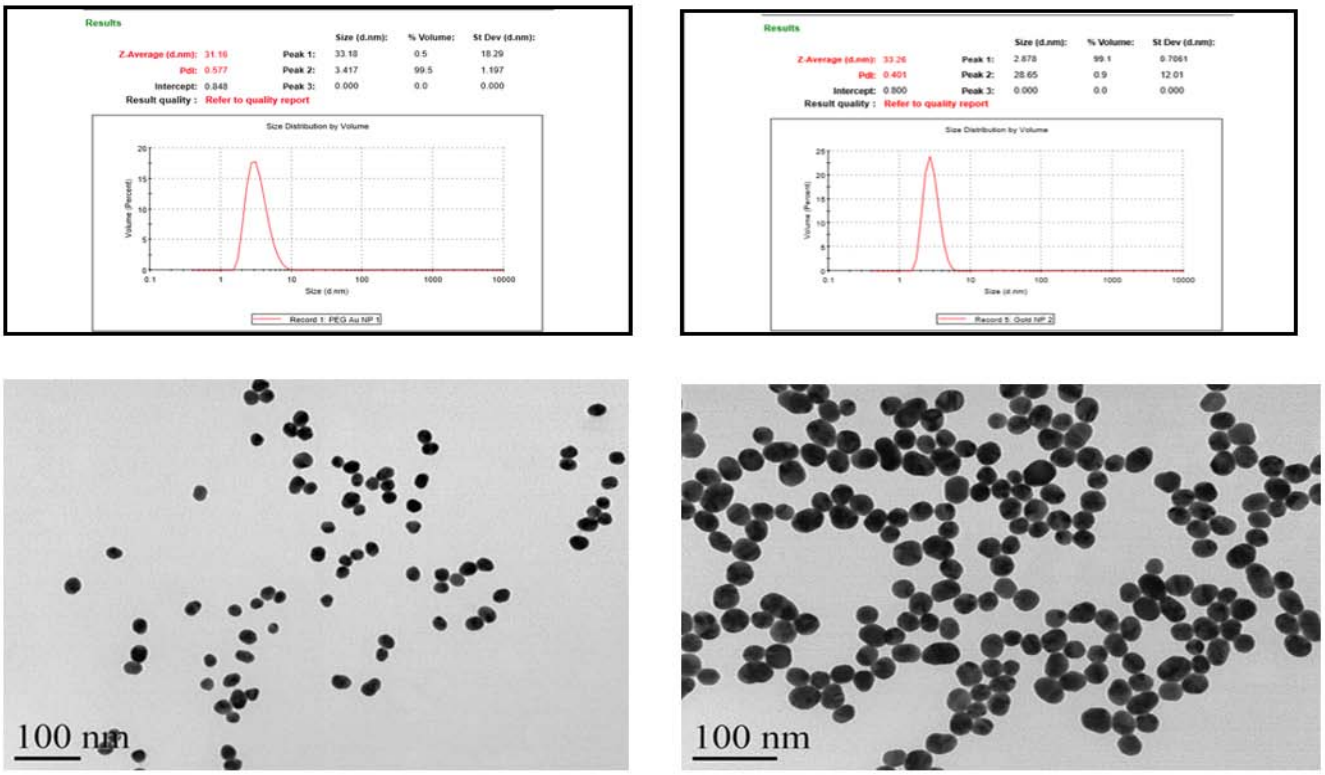

Figure 1: Analysis of non-coated and PEG coated gold nanoparticles size by DLS and TEM. Representative DLS images (A) and size distribution by TEM (B) after 24h incubation in cell- free culture medium. Scale bars represent 100 nm (1B and 2B) 27.

Table 1: Size distribution of AuNPs measured by DLS and TEM.

Measuring Method	Particle Size (nm)	
	AuNP	PEG-AuNP
DLS	28.6±0.8	33.2±1.2
TEM	25.8±5.4	35.3±3.6

of 25nm AuNPs after addition PEG increasing aggregation [35]. TEM images were obtained with a JOEL 1011 TEM system calibrated at 100keV and 300kX magnification. Among the two structures analyzed, PEG-coated AuNPs (Type 1) agglomerated in the 25-30 nm size range, while uncoated AuNPs (Type 2) were mainly spherical in the same range of 20-25 nm.

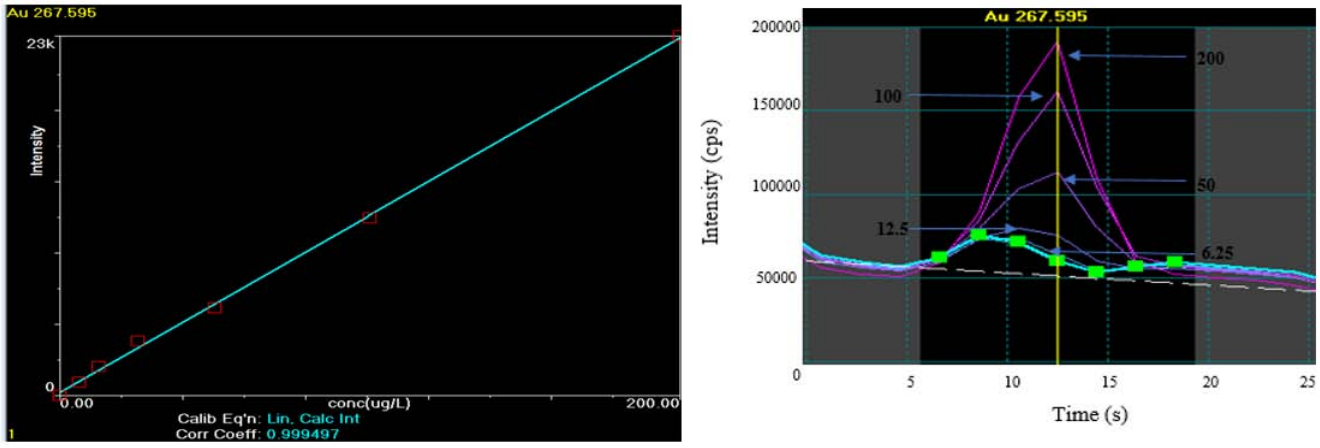

Figure 2: Plot of intensity vs. concentration of gold nanoparticles standards (0, 6.25, 12.5, 25, 50, 100, 200 µM) as determined with the Optima 8000 and WinLab ICP-OES Software.

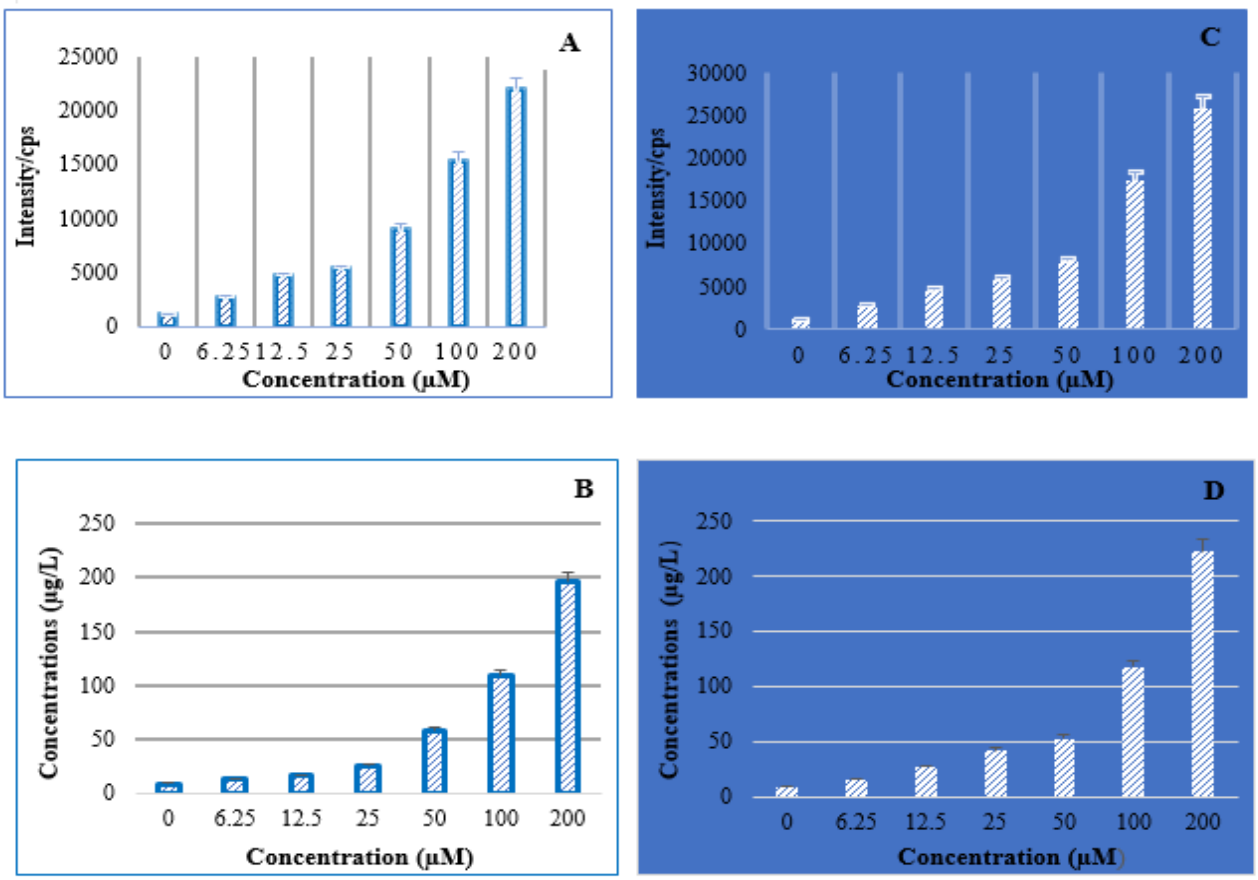

Figure 3: Sample data representing the concentrations of uncoated (A, B) and PEG coated Au nanopaticles (C, D) measured at 267.595 nm after 24 hour exposure of HK-2 cells.

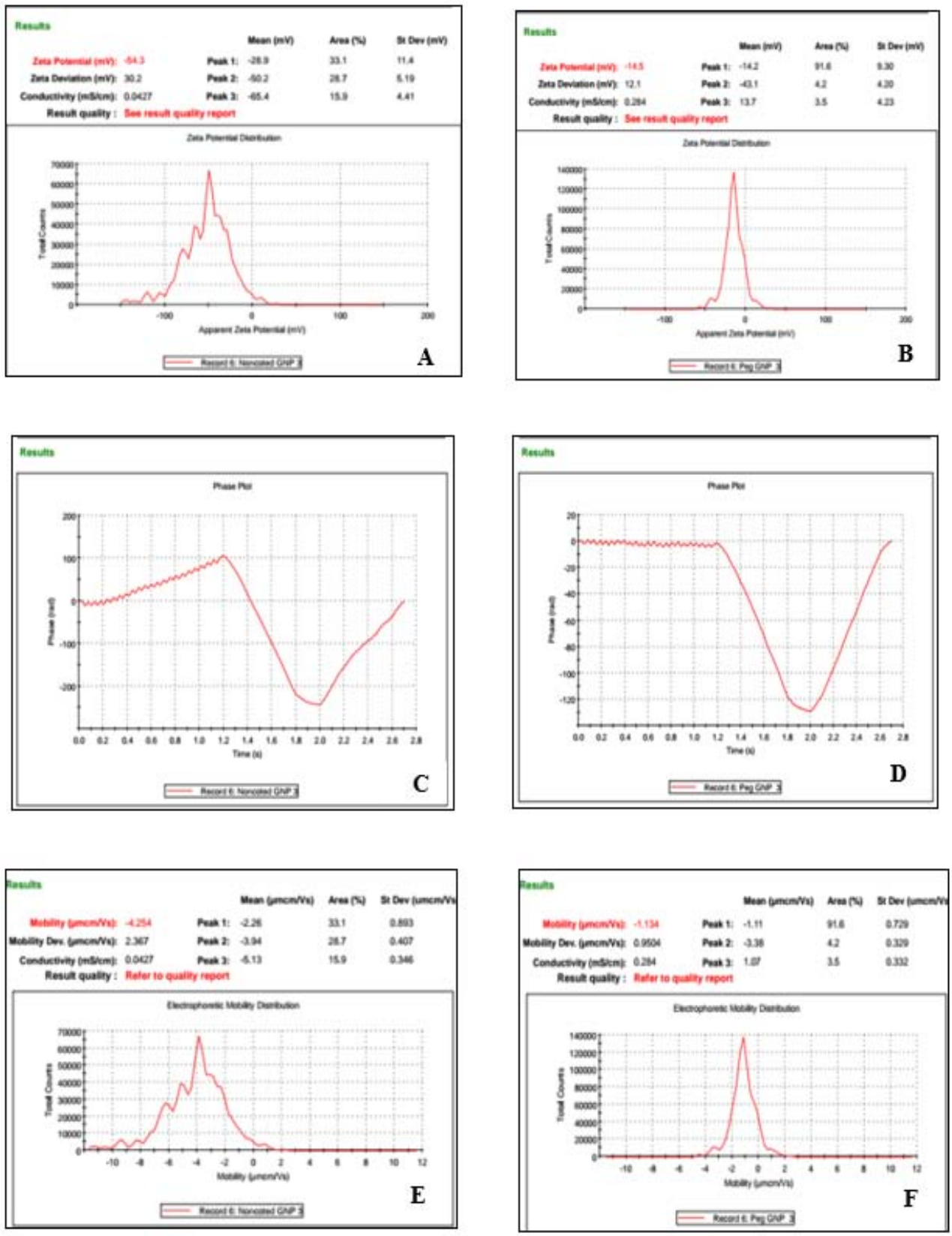

Figure 4: Comparison graphs of zeta potential, phase plot, and electrophoretic mobility distribution between uncoated AuNPs (A, C, E) and PEG coated Au nanoparticles (B, D, F).

ICP/OES analysis of gold nanoparticles

In order to analyze gold nanoparticles by ICP/OES, an effective *in-vitro* method had to be modified to accommodate HK-2 cells treated with PEG-coated or uncoated AuNPs. The instrumental method was setup to analyze AuNP in axial mode which allows for analysis of the AuNP observed in the excitation channel covering the entire axis of the plasma field. An optical interface located next to the plasma releases argon gas to cool itself, and to direct parts of the plasma form the interface's opening through which light passes into the optical chamber. This axial-view design allows a large amount of light into the optical chamber, and thus allowing large amounts of information available to process. This creates a system that produces maximum sensitivity in detecting trace element emissions. ICP-OES can now be used as a new tool for characterizing AuNPs in bioanalytical applications. A calibration curve was determined by using Au standard (SCP Science) 1003 + 3 µg/mL in 10% HCL. This standard was made using a 1000 ppb stock solution diluted in ultra with pure water. The wavelength used to measure Au was 267.595nm. Figure 2 represents ICP-OES calibration results with a concentration range of 0-200ppb. The uptake effectiveness was determined quantitatively together with the concentration levels of gold ions in AuNP-treated cells. Figure 3 shows the particle concentrations for both PEG-coated and uncoated AuNPs in comparison to the known particle amounts in standard samples. Their strong correlation demonstrates the accuracy of the measurements by ICP/OES analysis.

Physiochemical properties of AuNPs

Properties and function are determined by the surface charge of the Au nanoparticle. Their charge has a direct correlation with nanoparticle toxicity which translates into the fact that, the more negatively charged the particle, the higher the potential for cellular toxicity. The uncoated AuNPs exhibited a negative zeta potential (-54.3 ± 3 mV) which demonstrates a higher probability for toxicity (Figure 4A) compared to a more positive (-14.5 ± 1 mV) zeta potential for PEG-coated AuNPs as shown in (Figure 4B). The PEG-coated AuNPs possess a lower negatively charge surface than uncoated AuNPs which makes them more stable and less receptive to surface modifications. The phase plot for the uncoated AuNPs displays an increase in phase frequency up to a 100 rads (Figure 4C) compared to a steady phase frequency of zero rads from 0 to 1.2 seconds which relates to PEG coated AuNP stability (Figure 4D). The electrophoretic mobility of the particle was assessed based on the mean phase shift with time. This is an indicator of the relative surface charge associated with nanoparticle attachment and stability. The mobility of the uncoated AuNPs showed a total count of (~7000) with (-4.254 ± 1.4µmcm/Vs) mobility (Figure 4E), whereas PEG-coated AuNPs were almost neutral (-1.134 ± 1.3µmcm/Vs) with a total count of (~14,000) which is double the amount of the uncoated particles (Figure 4F). This verifies the stability of the PEG-coated AuNPs compared to the unstable uncoated AuNPs.

Trypan blue exclusion assay

This test protocol is generally used as one of the major assessment of cytotoxicity. It was performed to measure the numbers of live versus dead cells after 24-hour treatment with AuNPs. PEG-coated nanoparticles displayed higher percentages of cell viability compared to uncoated AuNPs as a function of AuNP concentrations (Figure 5).

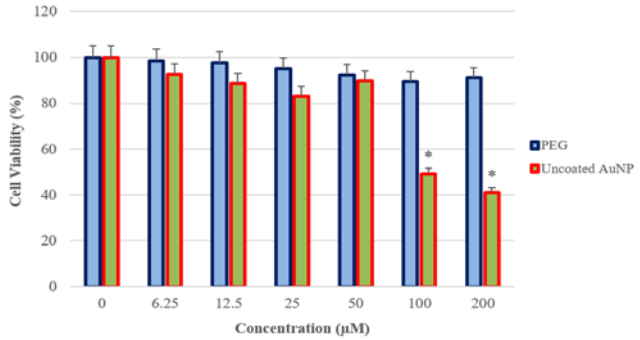

Figure 5: Cell viability in human kidney cells (HK-2) cells after 24h exposure to different concentrations (6.25, 12.5, 25, 50, 100, 200 µM) of PEG coated and uncoated AuNPs. The cell viability was evaluated with the trypan blue assay and the results were presented as the percentages of cell viability. Data are presented as the mean + standard deviation (SD) of three independent experiments. *p <0.05 and **p <0.01 in comparison to untreated controls using Student's t-test.

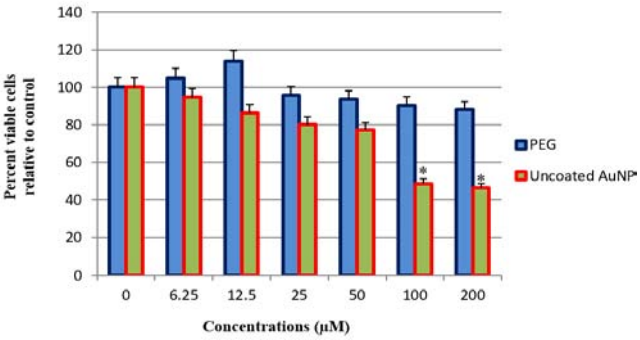

Figure 6: Cytotoxicity assessment of uncoated and PEG coated AuNPs on HK-2 human kidney cells, by the cyto tox glo luminescence assay. The PEG-coated AuNPs show no significant difference (p >0.05) in the viability of cells compared to the control, while uncoated AuNPs show significant reduction (p <0.05) in cell viability at 100 and 200 µM treatment.

Cyto Tox-Glo assay

The cytotoxicity of PEG-coated or uncoated AuNPs to HK-2 kidney cells was also investigated using the Cyto Tox-Glo assay. This assay detects both the dead and live cell populations found in a sample by measuring luminescence with a filter setting of 590 emissions and a gain adjusted to 3600. The data were collected as relative light units (RLU). (Figure 6) presents the results of Cyto Tox-Glo luminescence assay. As indicated on this figure, PEG-coated AuNPs show no significant differences (p >0.05) in cell viability compared to the controls, even at the highest test concentration of 200µM. Uncoated AuNPs show significant reduction (p <0.05) in the viability of HK-2 cells at 100 and 200µM treatment, compared to the controls.

Reactive oxygen species (ROS) assessment using 2',7'-dichlorofluorescein (H2DCF)

ROS production is considered as one of the major inducers of nanotoxicity. This is mainly because a higher amount of ROS distrupts the oxidative balance in the cell. There are many forms of intracellular ROS that exist in the cellular environment including superoxide (O_2^-), hydoxyl radical (HO·), hydrogen peroxide (H_2O_2), and peroxy radical (ROO·). Overproduction of ROS can result in impairment of normal

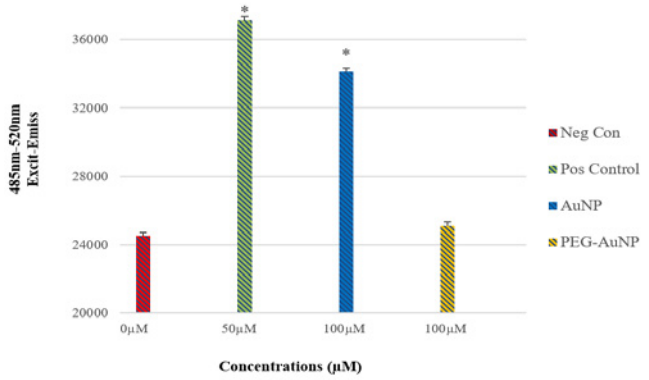

Figure 7: PEG coated and uncoated AuNP-induced ROS in HK-2 cells. Cells were treated with 100µM concentrations of PEG coated and uncoated AuNPs as well as to 50µm of tert-butyl hydrogen peroxide (TBHP) that was used as the positive control. Both uncoated AuNP (100µM) and TBHP (50µM) showed significant increase in ROS production compared to the negative control, while PEG coated AuNP (100µM) did not show any significant difference.

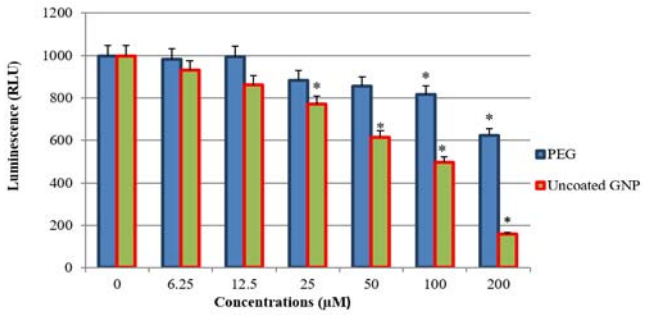

Figure 8: Effects of PEG-coated and uncoated AuNPs on the levels of GSH in HK-2 cells. Cells were treated with NPs at different concentrations and GSH was measured as described in the Materials and Methods section. A statistically significant difference ($p < 0.05$) in GSH levels was observed in AuNP-treated cells compared to the controls.

cellular activities by reacting with lipids, proteins and nucleic acids. In this experiment, we investigated the formation of (ROS) within HK-2 cells treated with LC50 concentrations of both PEG-coated and uncoated AuNPs. We found a statistically significant ($p < 0.05$) induction of intracellluar ROS in HK-2 cells treated for 24 hours with uncoated AuNPs whereas the PEG-coated AuNPs demonstrated low levels of ROS formation compared to the negative control (Figure 7).

Measurement of glutathione (GSH)

Further evidence of oxidative stress is indicated by the decrease production of glutathione (GSH) levels either by oxidation to glutathione disulfide (GSSG) or reaction with the thiol group. Data generated from the GSH-Glo assay indicated that the concentration levels of glutathione in HK-2 cells decreased significantly after 24hr exposure; with uncoated AuNPs showing more reduction in GSH concentrations compared to PEG-coated AuNPs (Figure 8).

Assessment of mitochondrial membrane potential (Δψm)

Since a change in Δψm is an essential parameter in apoptosis/necroptosis associated with ROS generation and oxidative stress, the examination of uncoated and PEG-coated AuNP exposure became necessary to ascertain any alteration in mitochondrial Δψm. The

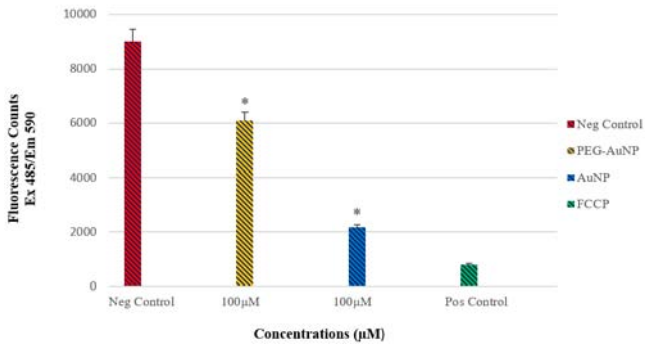

Figure 9: Effects of uncoated AuNP and PEG coated AuNP on the mitochondrial membrane potential in HK-2 cells. Cells were treated with AuNP for 24 hours and the mitochondrial membrane potential was determined using a cationic dye (JC-1) as described in the Materials and Methods section. Error bars represent mean ± SD (n=3) *P <0.05 indicates a statistically significant difference was observed compared to the control.

uncoated AuNPs exhibited a three-fold reduction in fluorescence counts compared to PEG-coated AuNPs representing a stronger depolarization of mitochondrial membrane potential (Figure 10). This result demonstrates the increase potential for oxidative stress displayed by uncoated AuNPs causing a mitochondrial damage by destabilizing the outer membrane and thereby disrupting the electron transport chain of the oxidative phosphorylation which may lead to apoptosis/necroptosis (Figure 9).

Measurement of genotoxicity using comet assay

Investigating the potential genotoxicity effects caused by gold nanoparticles, coated and uncoated, is essential due to their ability to interact with biological systems. This interaction interferes with normal cellular functions such as signaling and metabolic pathways that have a direct link to oxidative DNA damage determined by DNA strand breaks (Figure 10 and 11).

Assessment of chromosomal aberrations

Evaluation of chromosomal aberrations typically involves the treatment of cells during S-phase (due to the sensitivity of cells at this point in the cell cycle) followed by treatment two to three hours before sampling, dividing cells are arrested at metaphase by adding colchicine (1µg/mL). Figure 12A and 12B describes examples of chromsome aberrations that occur after cytogenetic damage. Such abnormalities illustrate the potential of test substances to induce a genotoxic damage. For instance, chromosome exchanges can result in dicentric formation, where the re-arrangement contains two centromeres and is readily visible, or a balanced translocation where the chromosomes may appear normal using conventional staining techniques and allow normal cell division. The light microscopy images using a low power objective (e.g. 10×) show the chromsomal differences between the AuNPs uncoated and PEG coated clearly demonstrating the levels of genotoxicity produced after a 24-hour incubation period. In many cases the chromosomes exhibited multiple aberrations which are more than seven aberrations per cell, or too many aberrations to permit accurate analysis. One hundred metaphases from each culture were analysed for chromosome aberrations, 50 per slide, making 200 per concentration of PEG-coated or uncoated AuPN. Only cells with 44-46 chromosomes were considered acceptable for analysis. Any cells with more than 46

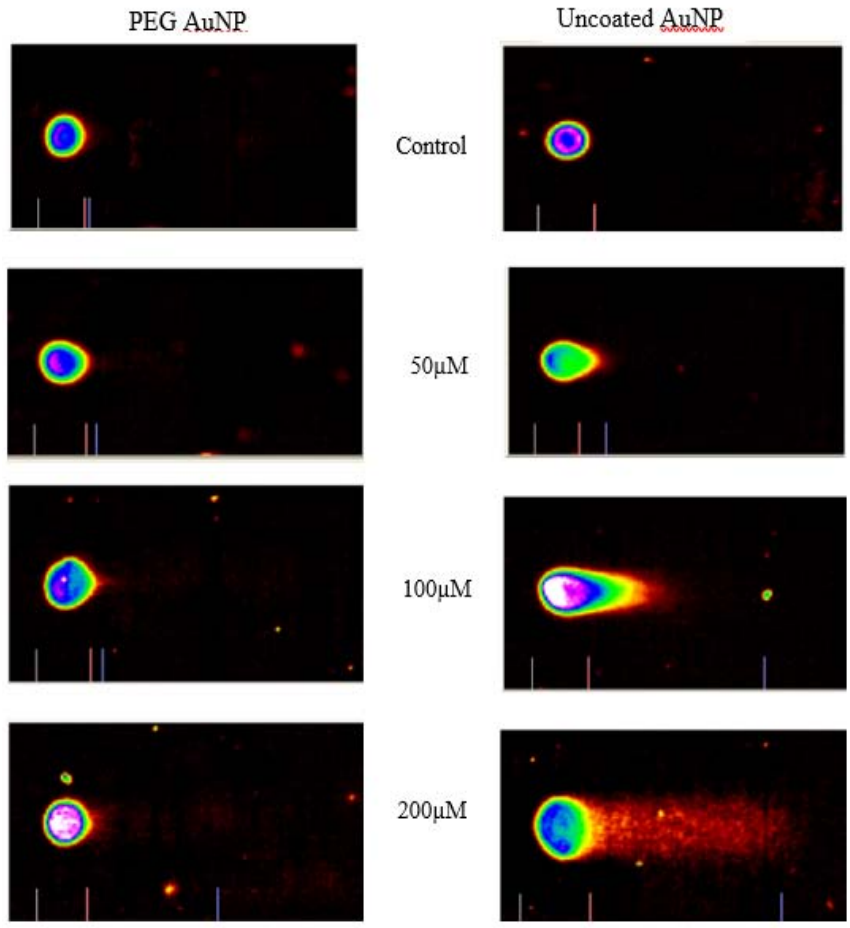

Figure 10: The comet assay is design to analyze DNA strand breaks and quantify the amount of DNA damage cause by 24-hour exposure to coated/uncoated Au nanoparticles. Cells were treated respectively with 50µM, 100µM and 200µM. Cells were stained with SyBr green and imaged with a Loats Comet assay system with an Olympus fluorescent microscope.

chromosomes (that is, polyploid, hyperdiploid, or endoreduplicated cells) were recorded separately and quantified if necessary.

Discussion

The wide use of nanoparticles in the medical field for diagnostics and therapeutic purposes has led to public concern over their potential toxicity to humans and the environment. The present study focuses on the characterization of uncoated and PEG-coated AuNP, and the evaluation of their cytotoxic and genotoxic effects and mechanisms of action in human kidney (HK-2) cells. In order to determine the size distribution and particle shape of both types of AuNPs, DLS and TEM were utilized, respectively. DLS measurements reported lower diameter profiles for PEG-coated AuNPs than those obtained by TEM, however DLS measurements for uncoated AuNPs revealed higher size distribution (Table 1). However, these differences can be explained by the differences in experimental conditions and instrumental analysis [36].

The ICP-OES gives us the technology capable of understanding the impact nanoparticle has on biological systems. In order to gain insight on how certain parameters affect the physiochemical properties of nanoparticles the ICP-OES can determine aggregation and colloidal stability of AuNPs which could lead to nanoparticle toxicity/biocompatibility [37]. ICP-OES analysis of gold ions in PEG-coated and uncoated AuNPs clearly indicates that gold nanoparticles were effectively up-taken by HK-2 cells. Many published studies have reported that the receptor-mediated endocytosis pathway plays a key role in AuNPs uptake by the cells [38,39]. It has also been pointed out that AuNPs in the size range of 25-50nm are highly up-taken in the endosomes and lysosomes of cells, while those less than 25nm or greater that 50nm are mainly found on the plasma membrane and hence, not easily absorbed into the cells.

It is evident from the physico-chemical data that the PEG-coated AuNPs displayed a higher biocompatible index than uncoated nanoparticles. Au NPs have been described to potentially induce toxicity by penetrating the nuclear compartment and binding to DNA [40]. Studies have shown enhance stability, as well as decreased hemolytic and cytotoxic activity of PEGylated AuNPs in comparison to their non-PEGylated variants. Surface charge changes by addition of PEG resulted in enhanced biocompatibility [41].

The gold nanoparticles we used were synthesized using trisodium citrate (reducing agent) and- the zeta potential for PEG-coated particles was 54.3 ± 2 mV less than uncoated AuNPs; demonstrating that PEG coating surrounding the gold nanoparticles provides a

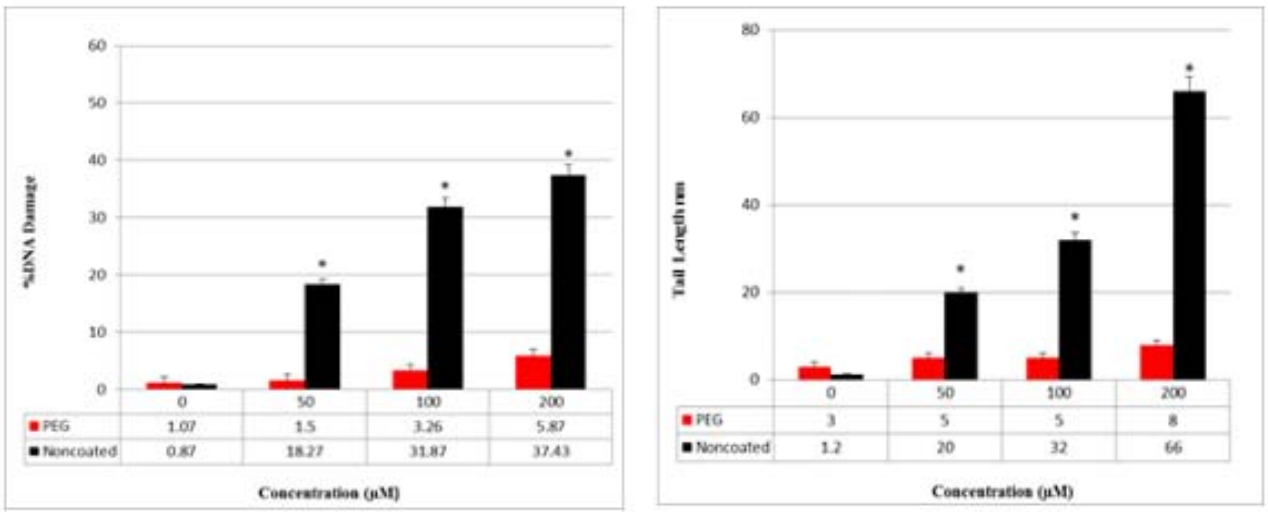

Figure 11: Data generated from these studies showed an increase in the mean percentage values of DNA cleavage and comet tail length. PEG AuNP resulted in a marginal (1.07%) insignificant increase ($p < 0.05$) of DNA damage compared to the AuNP treated cells (37.4%). It is evident that uncoated AuNPs exhibited genotoxic effects in a concentration-dependent manner.

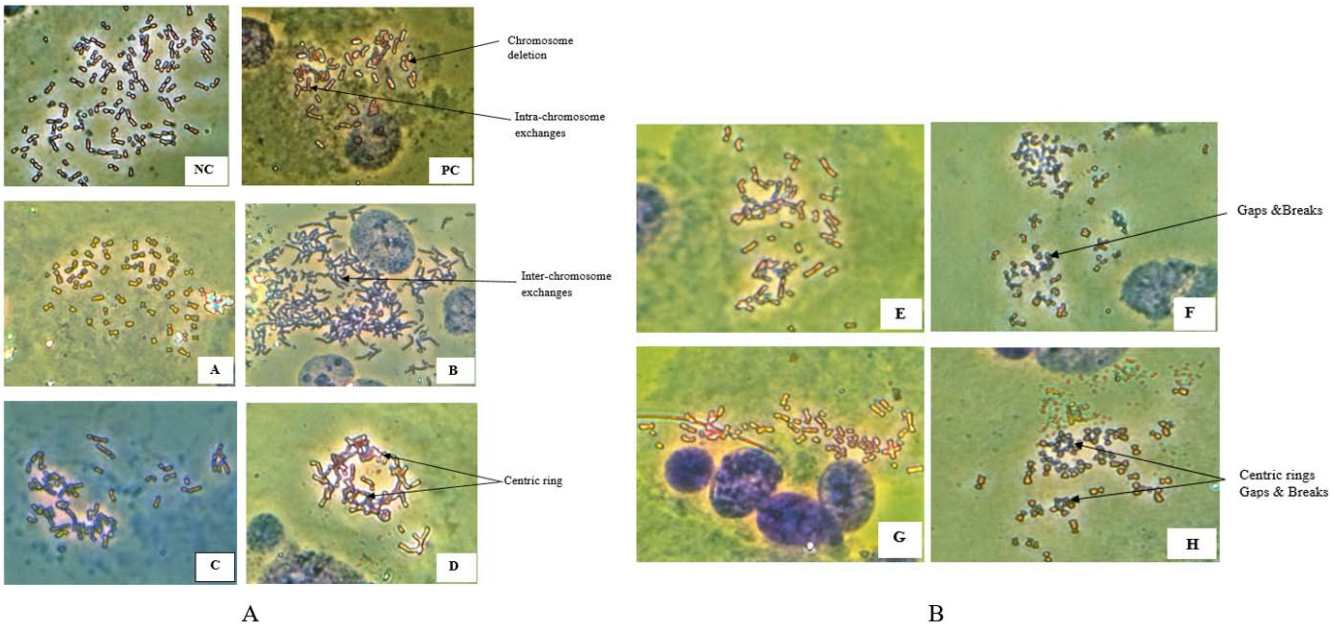

Figure 12: A & B: Images of human kidney chromosomes from cells after 24 hour exposure to coated/uncoated AuNP. Cells were fixed, placed on slides and stained with 4% Giemsa to assess mitotic inhibition. No treatment is Negative Control (NC), Cyclophosphamide (CPA) 15µg/mL represents positive control (PC). Images (A), (C), (E), and (G) are for PEG-coated AuNPs at concentrations of 6.25, 25, 50, 100 µM respectively. Images (B), (D), (F) and (H) coincide with uncoated AuNPs demonstrating increasing genotoxic effects in a concentration-dependent manner.

protective function in reducing the cytotoxic effects of uncoated "naked" gold nanoparticles.

The cell viability of HK-2 cells was examined by trypan blue exclusion assay after treatment with both types of AuNPs. The results suggest that uncoated AuNPs were cytotoxic to HK-2 cells and that their toxic effect was concentration-dependent. These results are consistent with similar studies that have been published on the toxicity results of gold nanoparticles. Paino et al. [42] reported that AuNP-induced cytotoxicity is highly influenced by the type of surface coating.

PEG-gold nanoparticle complexes did not exhibit cytotoxicity on HK-2 cells at concentrations up to 200µM. A similar finding was obtained by Lopez-Chavesv et al. [43]. Researchers reported that HepG2 cells experienced oxidative stress-induced damage with increased tissue phospholipid and protein oxidation.

Cell cytotoxicity was also determined by the Cytotox-Glo assay which was employed to measure a distinct protease activity associated with cytotoxicity of gold nanoparticles at different concentrations.

The cytotoxicity results from the Cytotox-Glo assay indicate that uncoated gold nanoparticles were toxic to HK-2 cells with a 50% lethal concentration (LC50) of 100μM. These results are consistent with the conclusion from a previous study demonstrating that AuNPs treatment compromises membrane integrity, thereby releasing protease components causing a disruption of metabolic pathways [44].

The results of our study also demonstrate that AuNP treatment at LC50 concentrations for 24 hr induced a significant level of ROS production in HK-2 cells. However, it was evident that the AuNPs encapsulated with PEG reduced ROS generation by decreasing surface reactivity and inhibiting the release of soluble metal components leading to a reduction in ROS production and subsequently decreasing oxidative stress in HK-2 cells, and reducing the toxic effects of AuNPs.

These findings are in support of results from previously published research indicating that ROS production is a major contributor to NPs toxicity. Pujalté et al. [45] reported a dose-dependent increase in ROS associated with the increase in particle reactivity and/or release of metal ions.

Glutathione (GSH) is one of the commonly evaluated biomarkers of oxidative stress, as changes in GSH concentration reflects the intracellular redox potential. ROS can cause a drop in GSH levels either by oxidation or reaction with the thiol group. Oxidative stress can also be evaluated in terms of glutathione (GSH) and glutathione disulfide (GSSG) ratio in the cell [46]. The data from GSH-Glo assay indicate a significant reduction in glutathione production in HK-2 cells by three-fold for uncoated AuNPs at a concentration of 200μM. Interestingly, the levels of GSH in cells treated with 200μM PEG-coated AuNPs were the same as those cells treated with 50μM uncoated AuNPs. Thus, uncoated AuNPs significantly decreased intracellular GSH concentrations. Other studies have reported similar results with other metallic nanomaterials; indicating that their action on GSH/GSSG represents an important mechanism of cytotoxicity induced by AuNPs [47].

Scientific evidence suggests that the mitochondrial membrane potential is one of the key biomarkers of the intrinsic pathway of apoptosis. The nanomaterial toxicity lead to loss of mitochondrial membrane permeability and therefore induces apoptosis by triggering cascade of intrinsic cell death pathway [48]. Also, excessive amount of ROS in the mitochondria can cause lipid peroxidation and loss of ΔΨM. As stated earlier, the uncoated AuNPs exhibited a three-fold reduction in fluorescence counts compared to PEG-coated AuNPs representing depolarization of mitochondrial membrane potential. This is a further evidence of the nanotoxicity of uncoated AuNPs causing oxidative stress with the increase in ROS production resulting in mitochondrial damage that may lead to necroptosis/cell death. Measurement of mitochondrial membrane potential in coated AuNPs shows their protective role [49].

It has been reported by Du et al. [50] that leaching of free metal ions alters gene expression as a consequence of high levels of ROS. Genotoxic effects are due to the perinuclear localization of the particles which may interfere with the process of transcription and translation. Cellular stress induced by AuNPs affects the activation ability of proteins by inhibiting cell-surface receptors involved in gene expression.

The alkaline single-cell gel electrophoresis assay was applied to HK-2 cells in order to measure the genotoxic effects resulting from the ability of denatured, cleaved DNA fragments to migrate out of the nucleoid under the influence of an electric field. The undamaged DNA migrates slower and remains within the nucleoid when a current is applied to the alkaline electrophoresis buffer.

The results clearly indicate the genotoxicity of uncoated AuNPs in a dose dependent manner whereas the opposite is true for PEG coated AuNPs revealing their protective role in reducing the genotoxic effects of gold nanoparticles. The data shows how the PEG AuNPs at its highest dose of 200μM presented with a marginal (4.8%) insignificant increase ($p > 0.05$), of DNA damage compared to the negative control cells that have not been treated with either AuNPs. The genotoxicity effect of HK-2 was expressed similarly to the comet assay using the *in vitro* mammalian chromosome aberration test. There is a definite difference between PEG coated and uncoated cytogenetic damage that was easily seen using light microscopy and Giemsa staining. Studies show that certain chemical agents cause chromosomal abberations leading to genotoxicity [51].

As stated by Clare [36] the distinction between an indirect-acting and a direct-acting genotoxin is important in predicting *in vivo* risk arising from a positive *in vitro* assay. For extrapolation to risk assessment for humans, the toxicokinetic profile, intended use and estimated exposure are important considerations, and the results need to be considered in context with the results of other genotoxicity tests. The results from the chromosome aberrations assay revealed a concentration dependent increase in gaps, breaks, intra and inter-chromosome exchanges with the uncoated AuNPs compared to PEG coated gold particles. The genotoxicity is significantly reduced in the PEG-coated HK-2 cells owing to their protective mechanism in lowering the AuNPs negative charge; producing a more stable and biocompatible gold nanoparticle.

Conclusion

In this study we used novel technologies such as DLS, zeta potential assessment, TEM, and ICP-OES to characterize the physico-chemical properties of PEG-coated and uncoated AuNPs, and conducted molecular studies to assess their cytotoxic and genotoxic effects on human kidney (HK-2) cells. Using ICP-OES, we demonstrated that uncoated AuNPs are uptaken into the cells and induce toxicity to cellular components while PEG-coated AuNPs show a minimal uptake/interaction and no toxicity. Trypan blue exclusion test and Cyto-Tox Glo data revealed that uncoated AuNPs cause a significant cytotoxicity in a concentration-dependent fashion, but induce a lower cytotoxicity at concentrations below the LC50 of 100μM. The treatment of cells with uncoated AuNPs increased ROS production and decreased both GSH and ΔΨM levels; indicating an increase in oxidative stress. PEG-coated AuNPs enhanced chemical stability, decreased negative charge and lowered cytotoxicity and oxidative stress. These factors contributed to a reduction in ROS formation and an enhanced effect on total glutathione content. PEG coating also prevented the depolarization of the mitochondrial membrane potential, and reduce the genotoxic stress, while uncoated

AuNPs induced significant DNA damage and caused a high number of chromosomal alterations including chromosome gaps, centric rings, breaks, deletions, and intra and inter-chromosome exchanges, in a concentration-dependent manner. Hence, PEG-coating decreases the positive charge of AuNPs leading to a reduction of binding and interaction with cell surface, as well as a reduction in particle uptake and toxicity to cellular components. In comparison with uncoated AuNPs, PEG-coated AuNPs were found to be more stable, biocompatible, and less cytotoxic and genotoxic; underscoring their potential use in therapeutic drug delivery for the eradication of cancer and other malignancies.

Declaration

Acknowledgements: This research was funded by NIH/NIMHD grant #G12MD007581 (RCMI-Center for Environmental Health), NIH/NIMHD grant #1U54MD015929 (RCMI Center for Health Disparities Research) and NSF grant #HRD 1547754 (CREST Center for Nanotoxicity Studies) at Jackson State University, Jackson, Mississippi, USA.

Author Contributions: Christian Rogers, Ph.D., conceived, designed, performed all of the experiments, analyzed most the data and also wrote the manuscript. Shaloam Dasari, Ph.D., edited the manuscript. Anita K. Patlolla, Ph.D., performed TEM analysis. Paul B. Tchounwou, Sc.D., provided financial support, supervised the research, and reviewed and proofread the manuscript. All authors reviewed and approved the final version of manuscript to be published.

References

1. Chandra P, Das D, Abdelwahab AA. Gold nanoparticles in molecular diagnostics and therapeutics. Digest Journal of Nanomaterials & Biostructures (DJNB). 2010; 5: 363-367.
2. Bracamonte MV, Bollo S, Labbé P, Rivas GA, Ferreyra NF. Quaternized chitosan as support for the assembly of gold nanoparticles and glucose oxidase: Physicochemical characterization of the platform and evaluation of its biocatalytic activity. Electrochimica acta. 2011; 56: 1316-1322.
3. Pissuwan D, Valenzuela SM, Cortie MB. Therapeutic possibilities of plasmonically heated gold nanoparticles. TRENDS in Biotechnology. 2006; 24: 62-67.
4. Nimesh S, Gupta N, Chandra R. Cationic polymer based nanocarriers for delivery of therapeutic nucleic acids. Journal of biomedical nanotechnology. 2011; 7: 504-520.
5. Zhang XD, Wu HY, Di Wu, Chang JH, Zhai ZB, Meng AM, et al. Toxicologic effects of gold nanoparticles *in vivo* by different administration routes. International journal of nanomedicine. 2010; 5: 771-781.
6. Li X, Zhou H, Yang L, Du G, Pai-Panandiker AS, Huang X, et al. Enhancement of cell recognition *in vitro* by dual-ligand cancer targeting gold nanoparticles. Biomaterials. 2011; 32: 2540-2545.
7. Fratoddi I, Venditti I, Cametti C, Russo MV. The puzzle of toxicity of gold nanoparticles. The case-study of HeLa cells. Toxicology Research. 2015; 4: 796-800.
8. Yah CS. The toxicity of Gold Nanoparticles in relation to their physiochemical properties. Biomedical Research. 2013; 24: 400-413.
9. Johnston HJ, Hutchison G, Christensen FM, Peters S, Hankin S, Stone V. A review of the *in vivo* and *in vitro* toxicity of silver and gold particulates: particle attributes and biological mechanisms responsible for the observed toxicity. Critical reviews in toxicology. 2010; 40: 328-346.
10. Lewinski N, Colvin V, Drezek R. Cytotoxicity of nanoparticles. Small. 2008; 4: 26-49.
11. Donaldson K, Stone V, Tran CL, Kreyling W, Borm PJ. Nanotoxicology. 2004; 61: 727-728.
12. Yu Y, Gao J, Jiang L, Wang J. Antidiabetic nephropathy effects of synthesized gold nanoparticles through mitigation of oxidative stress. Arabian Journal of Chemistry. 2021; 14: 103007.
13. Ding F, Li Y, Liu J, Liu L, Yu W, Wang Z, et al. Overendocytosis of gold nanoparticles increases autophagy and apoptosis in hypoxic human renal proximal tubular cells. International journal of nanomedicine. 2014; 9: 4317-4330.
14. Goodman CM, McCusker CD, Yilmaz T, Rotello VM. Toxicity of gold nanoparticles functionalized with cationic and anionic side chains. Bioconjugate chemistry. 2004; 15: 897-900.
15. Møller P, Jacobsen NR, Folkmann JK, Danielsen PH, Mikkelsen L, Hemmingsen JG, et al. Role of oxidative damage in toxicity of particulates. Free radical research. 2010; 44: 1-46.
16. Platel A, Carpentier R, Becart E, Mordacq G, Betbeder D, Nesslany F. Influence of the surface charge of PLGA nanoparticles on them *in vitro* genotoxicity, cytotoxicity, ROS production and endocytosis. Journal of Applied Toxicology. 2016; 36: 434-444.
17. L'azou B, Jorly J, On D, Sellier E, Moisan F, Fleury-Feith J, et al. *In vitro* effects of nanoparticles on renal cells. Particle and fibre toxicology. 2008; 5: 1-4.
18. Kermanizadeh A, Vranic S, Boland S, Moreau K, Baeza-Squiban A, Gaiser BK, et al. An *in vitro* assessment of panel of engineered nanomaterials using a human renal cell line: cytotoxicity, pro-inflammatory response, oxidative stress and genotoxicity. BMC nephrology. 2013; 14: 96.
19. Sen GT, Ozkemahli G, Shahbazi R, Erkekoglu P, Ulubayram K, Kocer-Gumusel B. The effects of polymer coating of gold nanoparticles on oxidative stress and DNA damage. International Journal of Toxicology. 2020; 39: 328-340.
20. Zhang XD, Wu HY, Di Wu, Chang JH, Zhai ZB, Meng AMet al. Toxicologic effects of gold nanoparticles *in vivo* by different administration routes. International journal of nanomedicine. 2010; 5: 771 -781.
21. Pissuwan D, Niidome T, Cortie MB. The forthcoming applications of gold nanoparticles in drug and gene delivery systems. Journal of controlled release. 2011; 149: 65-71.
22. Alkilany AM, Murphy CJ. Toxicity and Cellular Uptake of Gold Nanoparticles: What We Have Learned So Far. In Nanomaterials and Neoplasms. Jenny Stanford Publishing. 2021; 657-698.
23. Simpson CA, Huffman BJ, Gerdon AE, Cliffel DE. Unexpected toxicity of monolayer protected gold clusters eliminated by PEG-thiol place exchange reactions. Chemical research in toxicology. 2010; 23: 1608-1616.
24. Naha PC, Chhour P, Cormode DP. Systematic *in vitro* toxicological screening of gold nanoparticles designed for nanomedicine applications. Toxicology *in Vitro*. 2015; 29: 1445-1453.
25. Patlolla AK, Kumari SA, Tchounwou PB. A comparison of poly-ethylene-glycol-coated and uncoated gold nanoparticle-mediated hepatotoxicity and oxidative stress in Sprague Dawley rats. International journal of nanomedicine. 2019; 14: 639-647.
26. Schmidt B, Loeschner K, Hadrup N, Mortensen A, Sloth JJ, Bender Koch C, et al. Quantitative characterization of gold nanoparticles by field-flow fractionation coupled online with light scattering detection and inductively coupled plasma mass spectrometry. Analytical Chemistry. 2011; 83: 2461-2468.
27. Pissuwan D, Niidome T, Cortie MB. The forthcoming applications of gold nanoparticles in drug and gene delivery systems. Journal of controlled release. 2011; 149: 65-71.
28. Bumah VV, Masson-Meyers DS, Awosika O, Zacharias S, Enwemeka CS. The viability of human cells irradiated with 470-nm light at various radiant energies *in vitro*. Lasers in Medical Science. 2021; 38: 1661-1670.
29. Niles AL, Moravec RA, Hesselberth PE, Scurria MA, Daily WJ, Riss TL. A

homogeneous assay to measure live and dead cells in the same sample by detecting different protease markers. Analytical biochemistry. 2007; 366: 197-206.

30. Krug HF editor. Quality Handbook Standard Procedures for Nanoparticle Testing. Nanommune. 2011: 142-143.

31. Skalska J, Dąbrowska-Bouta B, Frontczak-Baniewicz M, Sulkowski G, Strużyńska L. A low dose of Nanoparticulate Silver induces mitochondrial dysfunction and autophagy in adult rat brain. Neurotoxicity Research. 2020; 38: 650-664.

32. Enea M, Pereira E, Peixoto de Almeida M, Araújo AM, Bastos MD, Carmo H. Gold nanoparticles induce oxidative stress and apoptosis in human kidney cells. Nanomaterials. 2020; 10: 995.

33. Kermanizadeh A, Vranic S, Boland S, Moreau K, Baeza-Squiban A, Gaiser BK, et al. An *in vitro* assessment of panel of engineered nanomaterials using a human renal cell line: cytotoxicity, pro-inflammatory response, oxidative stress and genotoxicity. BMC nephrology. 2013; 14: 96.

34. Clare G. The *in vitro* mammalian chromosome aberration test. In Genetic Toxicology. Springer, New York, NY. 2012; 817: 69-91.

35. Albanese A, Chan WC. Effect of gold nanoparticle aggregation on cell uptake and toxicity. ACS nano. 2011; 5: 5478-5489.

36. Ito T, Sun L, Bevan MA, Crooks RM. Comparison of nanoparticle size and electrophoretic mobility measurements using a carbon-nanotube-based coulter counter, dynamic light scattering, transmission electron microscopy, and phase analysis light scattering. Langmuir. 2004; 20: 6940-6945.

37. Donahue ND, Francek ER, Kiyotake E, Thomas EE, Yang W, Wang L, et al. Assessing nanoparticle colloidal stability with single-particle inductively coupled plasma mass spectrometry (SP-ICP-MS). Analytical and Bioanalytical Chemistry. 2020; 412: 5205-5216.

38. Dykman LA, Khlebtsov NG. Uptake of engineered gold nanoparticles into mammalian cells. Chemical reviews. 2014; 114: 1258-1288.

39. Barrios-Gumiel A, Sanchez-Nieves J, Pedziwiatr-Werbicka E, Abashkin V, Shcharbina N, Shcharbin D, et al. Effect of PEGylation on the biological properties of cationic carbosilane dendronized gold nanoparticles. International journal of pharmaceutics. 2020; 573: 118867.

40. Soenen SJ, Rivera-Gil P, Montenegro JM, Parak WJ, De Smedt SC, Braeckmans K. Cellular toxicity of inorganic nanoparticles: common aspects and guidelines for improved nanotoxicity evaluation. Nano today. 2011; 6: 446-465.

41. Pędziwiatr-Werbicka E, Gorzkiewicz M, Horodecka K, Lach D, Barrios-Gumiel A, Sánchez-Nieves J, et al. PEGylation of Dendronized Gold Nanoparticles Affects Their Interaction with Thrombin and siRNA. The Journal of Physical Chemistry B. 2021; 125: 1196-1206.

42. Paino IM, Marangoni VS, de Oliveira RD, Antunes LM, Zucolotto V. Cyto and genotoxicity of gold nanoparticles in human hepatocellular carcinoma and peripheral blood mononuclear cells. Toxicology letters. 2012; 215: 119-125.

43. Lopez-Chaves C, Soto-Alvaredo J, Montes-Bayon M, Bettmer J, Llopis J, Sanchez-Gonzalez C. Gold nanoparticles: distribution, bioaccumulation and toxicity. *In vitro* and *in vivo* studies. Nanomedicine: Nanotechnology, Biology and Medicine. 2018; 14: 1-2.

44. Seong M, Lee DG. Reactive oxygen species-independent apoptotic pathway by gold nanoparticles in Candida albicans. Microbiological research. 2018; 207: 33-40.

45. Pujalté I, Passagne I, Daculsi R, de Portal C, Ohayon-Courtès C, L'Azou B. Cytotoxic effects and cellular oxidative mechanisms of metallic nanoparticles on renal tubular cells: impact of particle solubility. Toxicology research. 2015; 4: 409-422.

46. Gao W, Xu K, Ji L, Tang B. Effect of gold nanoparticles on glutathione depletion-induced hydrogen peroxide generation and apoptosis in HL7702 cells. Toxicology letters. 2011; 205: 86-95.

47. Gallud A, Klöditz K, Ytterberg J, Östberg N, Katayama S, Skoog T, et al. Cationic gold nanoparticles elicit mitochondrial dysfunction: A multi-omics study. Scientific reports. 2019; 9: 4366.

48. Sanderson TH, Reynolds CA, Kumar R, Przyklenk K, Hüttemann M. Molecular mechanisms of ischemia-reperfusion injury in brain: pivotal role of the mitochondrial membrane potential in reactive oxygen species generation. Molecular neurobiology. 2013; 47: 9-23.

49. Du R, Niu W, Hong H, Huo S. Nanotoxicity and regulatory aspects in musculoskeletal regeneration. In Nanoengineering in Musculoskeletal Regeneration. Academic Press. 2020; 197-235.

50. Hilliard CA, Armstrong MJ, Bradt CI, Hill RB, Greenwood SK, Galloway SM. Chromosome aberrations *in vitro* related to cytotoxicity of nonmutagenic chemicals and metabolic poisons. Environmental and molecular mutagenesis. 1998; 31: 316-326.

51. Britain G. Committee on Mutagenicity of Chemicals in Food. CP at E. 2000.